Benchmark 3D: the VAG scheme*

Robert Eymard, Cindy Guichard and Raphaèle Herbin

1 Presentation of the scheme

Let Ω be a bounded open domain of $\mathbb{R}^3$, let $f \in L^2(\Omega)$ and let Λ be a measurable function from Ω to the set $\mathscr{M}_3(\mathbb{R})$ of 3×3 matrices, such that for a.e. $x \in \Omega$, $\Lambda(x)$ is symmetric, and such that the set of its eigenvalues is included in $[\underline{\lambda}, \overline{\lambda}]$, where $0 < \underline{\lambda} \leq \overline{\lambda}$. We wish to approximate the function u solution of

$$u \in H_0^1(\Omega) \text{ and } \forall v \in H_0^1(\Omega), \int_\Omega \Lambda(x)\nabla u(x) \cdot \nabla v(x) \mathrm{d}x = \int_\Omega f(x)v(x)\mathrm{d}x, \qquad (1)$$

by the approximate gradient scheme [4, 2] which reads:

$$U \in X_{\mathscr{D}}, \ \forall V \in X_{\mathscr{D}}, \ \int_\Omega \Lambda(x)\nabla_{\mathscr{D}} U(x) \cdot \nabla_{\mathscr{D}} V(x) \mathrm{d}x = \int_\Omega f(x)\Pi_{\mathscr{D}} V(x)\mathrm{d}x, \qquad (2)$$

where $\Pi_{\mathscr{D}}$ is a reconstruction operator and $\nabla_{\mathscr{D}}$ a discrete gradient operator which act on the discrete functional space $X_{\mathscr{D}}$, where the index $\mathscr{D}$ denotes the discretization; these operators are defined as defined as follows:

1. $\mathscr{M}$ is the set of control volumes, that are disjoint open subsets of Ω such that $\bigcup_{K \in \mathscr{M}} \overline{K} = \overline{\Omega}$, $\mathscr{V} = \mathscr{V}_{int} \cup \mathscr{V}_{ext}$ is the set of vertices of the mesh; any element K of $\mathscr{M}$ is defined by its vertices $s \in \mathscr{V}_K$, its faces $\sigma \in \mathscr{F}_K$; each face is also defined by the set of its vertices $s \in \mathscr{V}_\sigma$, using a suitable geometric definition for

R. Eymard
Université Paris-Est, e-mail: robert.eymard@univ-mlv.fr

C. Guichard
IFP Energies nouvelles and Université Paris-Est, e-mail: guichard@ifpenergiesnouvelles.fr

R. Herbin
Université Aix-Marseille, e-mail: Raphaele.Herbin@latp.univ-mrs.fr

* Work supported by Groupement MOMAS and ANR VFSitCom

the resulting surface in the case of non-planar faces; we assume that Λ is constant on all $K \in \mathscr{M}$, and we denote by Λ_K its value in K;
2. the set of discrete unknowns $X_{\mathscr{D}}$ is the finite dimensional vector space on $\mathbb{R}$, containing all real families $U = ((u_K)_{K\in\mathscr{M}}, (u_s)_{s\in\mathscr{V}})$, such that $u_s = 0$ if $s \in \mathscr{V}_{\rm ext}$;
3. the mapping $\Pi_{\mathscr{D}} : X_{\mathscr{D}} \to L^2(\Omega)$ maps $U = ((u_K)_{K\in\mathscr{M}}, (u_s)_{s\in\mathscr{V}}) \in X_{\mathscr{D}}$ to the piecewise constant function $u_{\mathscr{D}} \in L^2(\Omega)$ equal to u_K on each cell $K \in \mathscr{M}$;
4. the mapping $\nabla_{\mathscr{D}} : X_{\mathscr{D}} \to L^2(\Omega)^3$ is the reconstruction of a gradient from the values $U = ((u_K)_{K\in\mathscr{M}}, (u_s)_{s\in\mathscr{V}}) \in X_{\mathscr{D}}$; different expressions for this reconstruction are proposed below, which all lead to convergent gradient schemes in the sense of [4, 2]. Their theoretical analysis is related to that of the SUSHI scheme [1, 3]. Detailed numerical results are given in this paper only using the method described in subsection 1.2; the differences obtained using the other expressions are commented in the last section.

The exterior faces are those of the form $\partial K \cap \partial\Omega$ for any boundary control volume K, and the interior faces are those of the form $\partial K \cap \partial L$ for two neighbouring control volumes K and L. For any face σ, we define a point x_σ, which is a barycentre with non-negative weights $\beta_{\sigma,s}$ of the elements of the set $\mathscr{V}_\sigma$ including all the vertices of the face, and the value u_σ is defined by

$$u_\sigma = \sum_{s\in\mathscr{V}_\sigma} \beta_{\sigma,s} u_s \text{ with } \sum_{s\in\mathscr{V}_\sigma} \beta_{\sigma,s} = 1.$$

In the next three subsections, we describe three ways of defining a gradient operator which satisfies the VAG requirements. The first gradient is constructed from the Stokes formula on the cells of the mesh (we call it the primal cell to distinguish it from further constructed cells), and requires a stabilization. The second gradient and third gradients are constructed on tetrahedral or octahedral sub–cells of the primal mesh, and are natively stable.

1.1 Stabilised gradient on the primal mesh cells

For a face $\sigma \in \mathscr{F}$, we denote by τ any triangular sub-face with vertices x_σ, s and s', where s and s' are two consecutive vertices of σ. The barycentre x_τ of each sub-face τ may thus be expressed by the following barycentric combination:

$$x_\tau = \sum_{s\in\mathscr{V}_\sigma} \beta_{\tau,s} s \text{ with } \sum_{s\in\mathscr{V}_\sigma} \beta_{\tau,s} = 1,$$

where $\beta_{\tau,s} \geq 0$ for all $s \in \mathscr{V}_\sigma$. We then define $\beta_{\tau,s} = 0$ for all $s \in \mathscr{V} \setminus \mathscr{V}_\sigma$. Next, we reconstruct a value u_τ at the point x_τ, by $u_\tau = \sum_{s\in\mathscr{V}_\sigma} \beta_{\tau,s} u_s$. Let $K \in \mathscr{M}$ be an element of the mesh. We denote by $\mathscr{T}_K$ the set of all sub-faces of the faces of K.

We first define, for $U = ((u_K)_{K\in\mathscr{M}}, (u_s)_{s\in\mathscr{V}})$, an approximation of the gradient on cell K:

$$\nabla_K U = \frac{1}{|K|} \sum_{\tau \in \mathscr{T}_K} |\tau| \, (u_\tau - u_K) n_{K,\tau} = \sum_{s \in \mathscr{V}_K} (u_s - u_K) v_{K,s}, \tag{3}$$

where we denote by

$$v_{K,s} = \frac{1}{|K|} \sum_{\tau \in \mathscr{T}_K} \beta_{\tau,s} |\tau| \, n_{K,\tau},$$

where $n_{K,\tau}$ is the unit normal vector to τ, outward to K, and $|\tau|$, $|K|$ are respectively the area and the volume of τ and K. We then define a partition $M_{K,s}$ of K (there is no need to define this partition precisely), such that $|M_{K,s}| = |K|/N_K$, where N_K is the number of vertices of K and we introduce

$$R_{K,s} U = u_s - u_K - \nabla_K U \cdot (s - x_K).$$

We then define, for a given $\gamma > 0$, the constant value $\nabla_{K,s} U$ in $M_{K,s}$:

$$\nabla_{K,s} U = \nabla_K u + \gamma R_{K,s} U v_{K,s}.$$

We finally define a piecewise constant gradient by $\nabla_{\mathscr{D}} U(x) = \nabla_{K,s} U$ for a.e. $x \in M_{K,s}$. This scheme is denoted by "VAG" in [5].

1.2 Piecewise constant gradient on octahedral sub-cells

For a given face σ of a control volume K and for any vertex s of σ, we respectively denote by s^- and s^+ the preceding and the following vertices of s in the face σ (defining any orientation on σ), and we consider the (degenerate) octahedron, denoted by $V_{K,\sigma,s}$ and depicted in Fig. 1, whose vertices are $A_1 = x_K$, $A_2 = x_\sigma$, $A_3 = \frac{1}{2}(s^- + s)$, $A_5 = s$, $A_6 = \frac{1}{2}(s^+ + s)$ and $A_4 = \frac{1}{2}(x_\sigma + s)$ (note that all these octahedra are disjoint, and that the union of their closure is $\overline{\Omega}$). The approximate values of U at the vertices of $V_{K,\sigma,s}$ are respectively $u_1 = u_K$, $u_2 = u_\sigma$, $u_3 = \frac{1}{2}(u_{s^-} + u_s)$, $u_5 = u_s$, $u_6 = \frac{1}{2}(u_{s^+} + u_s)$ and $u_4 = \frac{1}{2}(u_\sigma + u_s)$ (the main diagonals of $V_{K,\sigma,s}$ are therefore (A_1, A_4), (A_2, A_5) and (A_3, A_6)). We then define the following approximate gradient:

$$\nabla_{K,\sigma,s} U = \sum_{i=1}^{3} (u_{i+3} - u_i) \frac{\overrightarrow{A_{i+1}A_{i+4}} \wedge \overrightarrow{A_{i+2}A_{i+5}}}{\mathrm{Det}(\overrightarrow{A_{i+1}A_{i+4}}, \overrightarrow{A_{i+2}A_{i+5}}, \overrightarrow{A_i A_{i+3}})}, \tag{4}$$

setting $A_7 = A_1$ and $A_8 = A_2$. We finally define a piecewise constant gradient by $\nabla_{\mathscr{D}} U(x) = \nabla_{K,\sigma,s} U$ for a.e. $x \in V_{K,\sigma,s}$. Remark that, denoting for simplicity V instead of $V_{K,\sigma,s}$, defining $\mathscr{F}_V$ as the set of the 8 triangular faces of V and $\mathscr{V}_\tau$ as the set of the 3 vertices of each triangular face τ of V, one may check that

$$\nabla_{K,\sigma,s} U = \frac{1}{|V|} \sum_{\tau \in \mathscr{F}_V} |\tau| n_{V,\tau} \Big(\frac{1}{3} \sum_{s \in \mathscr{V}_\tau} u_s \Big). \tag{5}$$

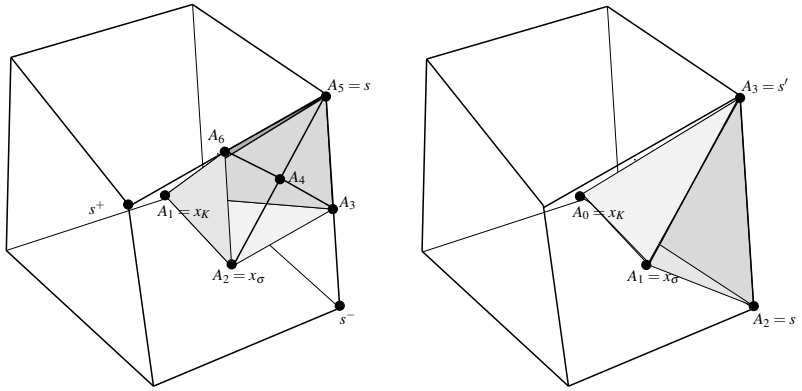

Fig. 1 The octahedral (left) and tetrahedral (right) cells for the definition of the gradient

We then set define $\nabla_K U$, used in the tables below, by

$$|K|\nabla_K U = \sum_{\sigma\in\mathscr{F}_K}\sum_{s\in\mathscr{V}_\sigma} |V_{K,\sigma,s}|\ \nabla_{K,\sigma,s}U.$$

This scheme is denoted by "VAGR" in [5].

1.3 Piecewise constant gradient on tetrahedral sub–cells

For a given face σ of a control volume K and for any pair of consecutive vertices (s,s') of σ, we consider the tetrahedron, denoted by $V_{K,\sigma,s,s'}$ and depicted in Fig. 1, whose vertices are $A_0 = x_K$, $A_1 = x_\sigma$, $A_2 = s$ and $A_3 = s'$ (note that all these tetrahedra are disjoint, and that the union of their closure is $\overline{\Omega}$). The approximate values of U at the vertices of $V_{K,\sigma,s,s'}$ are respectively $u_0 = u_K$, $u_1 = u_\sigma$, $u_2 = u_s$ and $u_3 = u_{s'}$. We then define the following approximate gradient:

$$\nabla_{K,\sigma,s,s'}U = \sum_{i=1}^{3}(u_i - u_0)\frac{\overrightarrow{A_0A_{i+1}}\wedge\overrightarrow{A_0A_{i+2}}}{\mathrm{Det}(\overrightarrow{A_0A_{i+1}},\overrightarrow{A_0A_{i+2}},\overrightarrow{A_0A_i})}, \tag{6}$$

where $A_4 = A_1$ and $A_5 = A_2$. We finally define a piecewise constant gradient by $\nabla_{\mathscr{D}}U(x) = \nabla_{K,\sigma,s,s'}U$ for a.e. $x \in V_{K,\sigma,s,s'}$. Remark that (5) also holds in this case, denoting V instead of $V_{K,\sigma,s,s'}$.

2 Numerical results

We provide the detailed numerical results obtained, using the scheme VAGR for computing the discrete gradient. In the numerical implementation, the values u_K are locally eliminated, and the unknowns of the linear solver are the values u_s. Denoting by $|\cdot|$ denotes the Euclidean norm, the norms used in the bench tables have been computed using the following formulae:

$$\text{normg} = \sum_{K\in\mathscr{M}} |K|\ |\nabla_K U|,$$

$$\text{erl2} = \left(\left(\sum_{K\in\mathscr{M}} |K|\,(u_K - u(x_K))^2\right) / \left(\sum_{K\in\mathscr{M}} |K|\,u(x_K)^2\right)\right)^{1/2},$$

$$\text{ergrad} = \left(\left(\sum_{K\in\mathscr{M}} |K|\,|\nabla_K U - \nabla u(x_K)|^2\right) / \left(\sum_{K\in\mathscr{M}} |K|\,|\nabla u(x_K)|^2\right)\right)^{1/2},$$

$$\text{ener} = \left(\left(\sum_{K\in\mathscr{M}} |K|\,|\nabla_K U - \nabla u(x_K)|^2_\Lambda\right) / \left(\sum_{K\in\mathscr{M}} |K|\,|\nabla u(x_K)|^2_\Lambda\right)\right)^{1/2},$$

setting, for any $K\in\mathscr{M}$, $|\xi|^2_\Lambda = \Lambda_K\xi\cdot\xi$ for all $\xi\in\mathbb{R}^3$.

• **Test 1 Mild anisotropy,** $u(x,y,z) = 1+\sin(\pi x)\sin\left(\pi\left(y+\frac{1}{2}\right)\right)\sin\left(\pi\left(z+\frac{1}{3}\right)\right)$ $\min = 0$, $\max = 2$**, Tetrahedral meshes**

i	nu	nmat	umin	uemin	umax	uemax	normg
1	488	6072	5.77E-02	2.03E-02	1.95E+00	1.99E+00	1.77E+00
2	857	11269	1.88E-02	6.84E-03	1.97E+00	1.99E+00	1.78E+00
3	1601	21675	2.19E-02	9.13E-03	1.98E+00	1.99E+00	1.79E+00
4	2997	41839	1.13E-02	5.52E-03	1.99E+00	2.00E+00	1.79E+00
5	5692	81688	8.73E-03	1.49E-03	1.99E+00	2.00E+00	1.79E+00
6	10994	160852	3.63E-03	1.83E-03	1.99E+00	2.00E+00	1.80E+00

i	nu	erl2	ratiol2	ergrad	ratiograd	ener	ratioener
1	488	1.76E-02	-	2.30E-01	-	2.28E-01	-
2	857	1.02E-02	2.93E+00	1.79E-01	1.35E+00	1.77E-01	1.35E+00
3	1601	6.79E-03	1.94E+00	1.44E-01	1.05E+00	1.42E-01	1.08E+00
4	2997	4.44E-03	2.03E+00	1.13E-01	1.14E+00	1.11E-01	1.17E+00
5	5692	2.79E-03	2.18E+00	9.02E-02	1.06E+00	8.89E-02	1.03E+00
6	10994	1.75E-03	2.13E+00	7.04E-02	1.13E+00	6.92E-02	1.15E+00

• **Test 1 Mild anisotropy,** $u(x,y,z) = 1+\sin(\pi x)\sin\left(\pi\left(y+\frac{1}{2}\right)\right)\sin\left(\pi\left(z+\frac{1}{3}\right)\right)$ $\min = 0$, $\max = 2$**, Voronoi meshes**

i	nu	nmat	umin	uemin	umax	uemax	normg
1	146	5936	7.54E-02	1.56E-01	2.15E+00	1.86E+00	1.14E+00
2	339	16267	-3.42E-01	1.79E-01	1.95E+00	1.81E+00	1.43E+00
3	684	37194	8.40E-04	2.67E-02	2.02E+00	1.93E+00	1.60E+00
4	1227	71069	-9.54E-02	1.20E-02	2.06E+00	1.91E+00	1.66E+00
5	2023	127883	-1.78E-02	3.85E-03	2.06E+00	1.97E+00	1.70E+00

i	nu	erl2	ratiol2	ergrad	ratiograd	ener	ratioener
1	146	1.82E-01	-	3.96E-01	-	4.05E-01	-
2	339	1.87E-01	-8.43E-02	2.49E-01	1.65E+00	2.53E-01	1.68E+00
3	684	9.92E-02	2.70E+00	1.55E-01	2.02E+00	1.62E-01	1.90E+00
4	1227	7.15E-02	1.68E+00	1.19E-01	1.35E+00	1.23E-01	1.42E+00
5	2023	4.74E-02	2.47E+00	9.56E-02	1.33E+00	9.92E-02	1.29E+00

• **Test 1 Mild anisotropy,** $u(x,y,z) = 1+\sin(\pi x)\sin\left(\pi\left(y+\frac{1}{2}\right)\right)\sin\left(\pi\left(z+\frac{1}{3}\right)\right)$ $\min = 0$, $\max = 2$**, Kershaw meshes**

i	nu	nmat	umin	uemin	umax	uemax	normg
1	729	15625	7.80E-02	3.03E-02	1.96E+00	1.96E+00	1.56E+00
2	4913	117649	1.72E-02	1.06E-02	1.98E+00	1.99E+00	1.68E+00
3	35937	912673	-2.58E-04	1.75E-03	1.99E+00	2.00E+00	1.74E+00
4	274625	7189057	-2.64E-04	7.14E-04	2.00E+00	2.00E+00	1.78E+00

i	nu	erl2	ratiol2	ergrad	ratiograd	ener	ratioener
1	729	9.17E-02	-	4.91E-01	-	4.84E-01	-
2	4913	5.53E-02	7.96E-01	3.09E-01	7.28E-01	2.84E-01	8.40E-01
3	35937	2.97E-02	9.38E-01	1.74E-01	8.70E-01	1.54E-01	9.22E-01
4	274625	1.22E-02	1.31E+00	7.40E-02	1.26E+00	6.44E-02	1.29E+00

• **Test 1 Mild anisotropy,** $u(x,y,z) = 1+\sin(\pi x)\sin\left(\pi\left(y+\frac{1}{2}\right)\right)\sin\left(\pi\left(z+\frac{1}{3}\right)\right)$ $\min = 0$, $\max = 2$**, Checkerboard meshes**

i	nu	nmat	umin	uemin	umax	uemax	normg
1	97	2413	-9.81E-02	1.54E-01	2.08E+00	1.85E+00	1.34E+00
2	625	22585	-1.90E-01	4.01E-02	2.19E+00	1.96E+00	1.70E+00
3	4417	188641	-6.12E-02	1.01E-02	2.06E+00	1.99E+00	1.78E+00
4	33025	1529617	-1.70E-02	2.54E-03	2.02E+00	2.00E+00	1.79E+00
5	254977	12295153	-4.33E-03	6.36E-04	2.00E+00	2.00E+00	1.80E+00

i	nu	erl2	ratiol2	ergrad	ratiograd	ener	ratioener
1	97	3.25E-01	-	4.37E-01	-	3.97E-01	-
2	625	1.11E-01	1.73E+00	1.50E-01	1.72E+00	1.52E-01	1.54E+00
3	4417	3.01E-02	2.00E+00	5.73E-02	1.47E+00	6.09E-02	1.41E+00
4	33025	7.92E-03	1.99E+00	2.51E-02	1.23E+00	2.77E-02	1.18E+00
5	254977	2.03E-03	2.00E+00	1.18E-02	1.11E+00	1.32E-02	1.08E+00

• **Test 2 Heterogeneous anisotropy,**
$u(x,y,z) = x^3y^2z + x\sin(2\pi xz)\sin(2\pi xy)\sin(2\pi z)$**,** $\min = -0.862$, $\max = 1.048$**,**
Prism meshes

i	nu	nmat	umin	uemin	umax	uemax	normg
1	3080	99634	-8.73E-01	-8.41E-01	1.10E+00	9.84E-01	1.53E+00
2	20160	710894	-8.25E-01	-8.39E-01	1.04E+00	1.01E+00	1.66E+00
3	63240	2301754	-8.52E-01	-8.59E-01	1.05E+00	1.03E+00	1.69E+00
4	144320	5340214	-8.53E-01	-8.57E-01	1.04E+00	1.03E+00	1.70E+00

i	nu	erl2	ratiol2	ergrad	ratiograd	ener	ratioener
1	3080	1.66E-01	-	1.40E-01	-	1.38E-01	-
2	20160	4.26E-02	2.17E+00	3.71E-02	2.13E+00	3.64E-02	2.13E+00
3	63240	1.93E-02	2.08E+00	1.67E-02	2.10E+00	1.63E-02	2.10E+00
4	144320	1.10E-02	2.05E+00	9.44E-03	2.06E+00	9.25E-03	2.07E+00

• **Test 3 Flow on random meshes,** $u(x,y,z) = \sin(2\pi x)\sin(2\pi y)\sin(2\pi z)$**,**
$\min = -1$, $\max = 1$**, Random meshes**

i	nu	nmat	umin	uemin	umax	uemax	normg
1	125	2197	-1.51E+00	-7.55E-01	1.68E+00	6.98E-01	1.53E+00
2	729	15625	-1.13E+00	-9.39E-01	1.21E+00	9.24E-01	2.99E+00
3	4913	117649	-1.08E+00	-9.85E-01	1.06E+00	9.82E-01	3.44E+00
4	35937	912673	-1.01E+00	-9.96E-01	1.01E+00	9.96E-01	3.56E+00

i	nu	erl2	ratiol2	ergrad	ratiograd	ener	ratioener
1	125	1.15E+00	-	6.19E-01	-	6.26E-01	-
2	729	2.56E-01	2.56E+00	2.02E-01	1.90E+00	1.81E-01	2.11E+00
3	4913	5.93E-02	2.30E+00	8.04E-02	1.45E+00	5.30E-02	1.93E+00
4	35937	1.49E-02	2.09E+00	3.45E-02	1.28E+00	1.74E-02	1.68E+00

• **Test 4 Flow around a well , Well meshes**

i	nu	nmat	umin	uemin	umax	uemax	normg
1	1248	27072	3.89E-01	4.29E-01	5.32E+00	5.32E+00	1.68E+03
2	2800	65184	2.41E-01	2.50E-01	5.33E+00	5.33E+00	1.65E+03
3	5889	143079	1.55E-01	1.57E-01	5.33E+00	5.33E+00	1.64E+03
4	12582	314964	1.18E-01	1.20E-01	5.33E+00	5.33E+00	1.63E+03
5	25300	645210	9.03E-02	9.09E-02	5.34E+00	5.34E+00	1.63E+03
6	45668	1178094	7.27E-02	7.30E-02	5.34E+00	5.35E+00	1.63E+03
7	79084	2055600	5.69E-02	5.68E-02	5.36E+00	5.36E+00	1.63E+03

i	nu	erl2	ratiol2	ergrad	ratiograd	ener	ratioener
1	1248	6.47E-03	-	5.78E-02	-	5.35E-02	-
2	2800	2.71E-03	3.23E+00	2.54E-02	3.05E+00	2.34E-02	3.08E+00
3	5889	1.19E-03	3.31E+00	1.23E-02	2.93E+00	1.15E-02	2.85E+00
4	12582	8.42E-04	1.37E+00	7.59E-03	1.91E+00	7.31E-03	1.79E+00
5	25300	4.47E-04	2.72E+00	5.10E-03	1.71E+00	4.95E-03	1.68E+00
6	45668	2.02E-04	4.03E+00	3.55E-03	1.83E+00	3.47E-03	1.80E+00
7	79084	1.75E-04	7.84E-01	3.26E-03	4.76E-01	3.19E-03	4.56E-01

• **Test 5 Discontinuous permeability,** $u(x,y,z) = \alpha_i \sin(2\pi x)\sin(2\pi y)\sin(2\pi z)$**,** $\min = 0$, $\max = 1$**, Locally refined meshes**

i	nu	nmat	umin	uemin	umax	uemax	normg
1	60	1148	-7.39E+02	-1.00E+02	7.39E+02	1.00E+02	1.24E+01
2	305	6825	-7.82E+01	-3.54E+01	7.82E+01	3.54E+01	5.20E+01
3	1881	46025	-9.90E+01	-7.89E+01	9.90E+01	7.89E+01	8.60E+01
4	13073	335601	-9.99E+01	-9.43E+01	9.99E+01	9.43E+01	9.56E+01
5	97185	2557793	-1.00E+02	-9.86E+01	1.00E+02	9.86E+01	9.80E+01

i	nu	erl2	ratiol2	ergrad	ratiograd	ener	ratioener
1	60	6.39E+00	-	1.60E+00	-	8.27E+00	-
2	305	1.19E+00	3.10E+00	5.97E-01	1.82E+00	6.01E-01	4.84E+00
3	1881	2.55E-01	2.55E+00	1.86E-01	1.92E+00	1.80E-01	1.99E+00
4	13073	6.10E-02	2.21E+00	5.96E-02	1.76E+00	4.78E-02	2.05E+00
5	97185	1.52E-02	2.08E+00	2.24E-02	1.46E+00	1.26E-02	2.00E+00

3 Comments on the results

The results obtained using (3) (VAG) instead of (4) (VAGR) are systematically less precise, except in the test5 case, where we obtained the following tables:

i	nu	nmat	umin	uemin	umax	uemax	normg
1	60	1148	-7.65E+02	-1.00E+02	7.65E+02	1.00E+02	6.76E+01
2	305	6825	-7.73E+01	-3.54E+01	7.73E+01	3.54E+01	4.65E+01
3	1881	46025	-9.02E+01	-7.89E+01	9.02E+01	7.89E+01	8.19E+01
4	13073	335601	-9.72E+01	-9.43E+01	9.72E+01	9.43E+01	9.43E+01
5	97185	2557793	-9.93E+01	-9.86E+01	9.93E+01	9.86E+01	9.77E+01

i	nu	erl2	ratiol2	ergrad	ratiograd	ener	ratioener
1	60	6.71E+00	-	7.32E+00	-	2.90E+01	-
2	305	9.53E-01	3.60E+00	6.91E-01	4.36E+00	6.76E-01	6.93E+00
3	1881	1.49E-01	3.05E+00	2.24E-01	1.85E+00	2.20E-01	1.85E+00
4	13073	3.27E-02	2.35E+00	6.17E-02	2.00E+00	5.95E-02	2.03E+00
5	97185	7.98E-03	2.11E+00	1.73E-02	1.90E+00	1.54E-02	2.02E+00

The results using (6) are very similar to those obtained using (4) (VAGR). For both (3) (VAG) and (4) (VAGR), we have chosen the conjugate gradient solver of the ISTL library with ILU(0) preconditioning with tolerance (or reduction factor) set to 10^{-10}. The following observations have been made on the computing times, using (3) (VAG) (we may expect that similar observations could be done with VAGR).

1. On the fourth Kershaw mesh and test 1, we obtain the following CPU times using the conjugate gradient solver of the PETSC library: with ILU(2), 33s, with ILU(1), 17s, with ILU(0), 10s, and with Jacobi, 11s, which shows that the ILU(0) preconditioning seems the fastest one on this case. Note that this computing time is depending on the unknown orderings. For the bench computations, we used the recursive domain decomposition ordering, which is the most efficient for direct solvers, and the respective computing times with PETSC CG+ILU(0) and with ISTL CG+ILU(0) are 10.3 and 11.2 s. Using the reverse Cuthill - McKee ordering, we respectively obtain 4.4 s and 15.3 s with PETSC CG+ILU(0) and ISTL CG+ILU(0).
2. The computing times, for the conjugate gradient solver of the PETSC library with ILU(1) preconditioning, in the test 1 case on tetrahedral meshes 2 to 5, have been approximately equal to 0.01, 0.03, 0.04, 0.08, and 0.16 s, showing the possibility to apply this method on much larger meshes.

Finally, we may not exclude that the systematic choice of computing the L^2 error with respect to the values in the control volumes instead of the vertex values, makes all these results somewhat pessimistic.

References

1. R. Eymard, T. Gallouët, and R. Herbin. Discretisation of heterogeneous and anisotropic diffusion problems on general non-conforming meshes, sushi: a scheme using stabilisation and hybrid interfaces. *IMA J. Numer. Anal.*, 30(4):1009–1043, 2010. see also http://hal.archives-ouvertes.fr/.

2. R. Eymard, C. Guichard, and R. Herbin. Small-stencil 3D schemes for diffusive flows in porous media. *submitted*, 2010. see also http://hal.archives-ouvertes.fr/.
3. R. Eymard, T. Gallouët and R. Herbin. Benchmark 3D: the SUSHI scheme *these proceedings*, 2011.
4. R. Eymard and R. Herbin. Gradient schemes for diffusion problem. *these proceedings*, 2011.
5. R. Eymard, G. Henry, R. Herbin, F. Hubert, R. Klöfkorn and G. Manzini. 3D Benchmark on Discretization Schemes for Anisotropic Diffusion Problems on General Grids. *these proceedings*, 2011.

The paper is in final form and no similar paper has been or is being submitted elsewhere.